LA-UR-16-26211
Approved for public release; distribution is unlimited.

Title: TA-54 (Area G) Risk Assessment from Extreme Fire Scenarios

Author(s): Linn, Rodman Ray
Koo, Eunmo
Honig, Kristen Ann
White, Judith Winterkamp
Funk, David John

Intended for: Report

Issued: 2016-08-11

TA-54 (Area G) Risk Assessment from Extreme Wildfire Scenarios

Rodman Linn, Eunmo Koo, Kristen Honig, Judith White, David Funk
Los Alamos National Laboratory
August 10, 2016

1. Background

Los Alamos National Laboratory (LANL) and surrounding areas have been exposed to at least four significant wildfires since 1977 and there have been numerous others within 50 miles of LANL. Based on this history, wildfires are considered a risk to LANL facilities and their contents. While many LANL facilities are at risk to wildfire to some degree, they are found in a wide variety of conditions, thus they have varying sensitivities to wildfires. Additionally, LANL facilities have various functions and different assets, so they have a wide range of values or consequences if compromised. Therefore, determining the risks and precautions that are warranted to mitigate these risks must be done on a case-by-case basis.

In an effort to assess possible wildfire risks to sensitive materials stored in a Perma-Con® in dome TA-54-0375[1], a conventional fire risk analysis was performed. This conventional risk analysis is documented in Engineering Evaluation Form AP-FIRE-001-FM1, which is dated 9/28/2015 and was titled 'Wildland Fire Exposure Evaluation for Building TA-54-0375' (Hall 2015). This analysis acknowledged that there was significant chance of wildfire in the vicinity of TA-54-0375, but the amount of combustible material surrounding the building was deemed low. The wildland fuels that were closest to the building were largely fine fuels and were not expected to have significant duration of heat release. The prevailing winds at this location are from the south and southwest and the nearest significant upwind fuels (tree crowns or unmown grasses) are at least 300 feet away. Based on these factors the conventional wildland fire risk to TA-54-0375 was deemed minimal, *"Acceptable As Is, No Action Required."* This risk evaluation was based on a combined assessment of low probability of wildfires arriving at the site from other directions (where higher fuel loadings might be present) as well as the effective setback of fuels in the direction that fire is expected to arrive from.

Due to the extreme concern over the fate of the contents of the Perma-Con® in TA-54-0375, risk management authorities and wildfire behavior experts at LANL felt that it was necessary to consider scenarios beyond the potentially anticipated fires analyzed in the conventional fire-risk evaluation described above. LANL risk management authorities decided to investigate the potential of circumstances where wildfires could pose a threat to the contents of the Perma-Con®, even if they were very unlikely. In these discussions, the probability of such a scenario

[1] 54-0375 is a structure consisting of a metal skeleton covered with a flame- or fire-resistant fabric. These structures are referred to as "domes."

developing was not considered as discerning criteria of whether a scenario should be addressed as long as it was seen as "possible".

The strategy to assess possible risk to the contents of the Perma-Con was determined to be as follows:

1. Identify extreme fire behavior scenarios that could provide high heat fluxes to the Perma-Con,

2. Use conservative scenario definitions whenever in doubt in order to consider a worst-case scenario,

3. Estimate convective and radiative heat fluxes to the Perma-Con using conservative means to account for wildfire's spatial heterogeneity, the details of which can not be exactly predicted, and

4. Perform a detailed heat transfer simulation of the contents of the Perma-Con using the estimated convective heat fluxes with a factor of safety for both peak fluxes as well as duration in order to determine the evolution of the temperature of the contents within the Perma-Con.

This final detailed analysis of the evolution of heat transfer and temperatures within the Perma-Con will be covered in a separate document.

With an understanding that there would be numerous details of a possible wildfire scenario that are impossible to define ahead of time (i.e. exact fuel conditions, the details of the wind fields, the precise shape of the fire perimeter as it approaches TA-54) and thus a fair amount of uncertainty in the inputs for wildfire simulations, LANL's approach to this risk analysis was to take a very conservative approach (worst-case scenario) to the wildfire modeling efforts and thus manage the possible consequences of the uncertainty.

2. Hypothetical extreme fire scenario

Through a series of brainstorming discussions, which were fed by recent hypothesis regarding the behavior of the Las Conchas wildfire during the early morning of June 27, 2011, a hypothetical extreme scenario was developed. In these extreme scenarios, significantly higher heat fluxes to the Perma-Con than in the scenarios considered under the Conventional Fire Risk Evaluation mentioned above were discussed as a possible phenomenon (or event).

The primary safety measure for the TA-54-0375 Perma-Con is the separation distance from fuels, especially from upwind fuels under prevailing winds. In the extreme hypothetical scenario, if multiple lines of fire were to interact, they could induce strong winds that might be capable of pulling heat from a wildfire over the mesa top. In this hypothetical scenario, fire in the canyons on both north and south sides of TA-54 and potentially on the mesa top west of TA-54, would induce a low pressure region between them as they compete for indrafts, as illustrated in Figure 1. The resulting low-pressure region between the fires and the imbalanced indrafts on either fire line could draw significant heat from a fire on the north side of the TA-54 mesa over the TA-54-0375 location. The result would be showers of firebrands and increased convective and radiative heat fluxes in the vicinity of the TA-54-0375 Perma-Con. Although the fabric forming the dome structure of building 0375 is fire resistant, it is possible that it could be melted to the point of being ineffective protection for the Perma-Con, especially in the context of showers of firebrands, which would be expected in the scenarios described above. Thus, for the development of a worst-case scenario, the dome was assumed as fully compromised (gone) when the fire arrives.

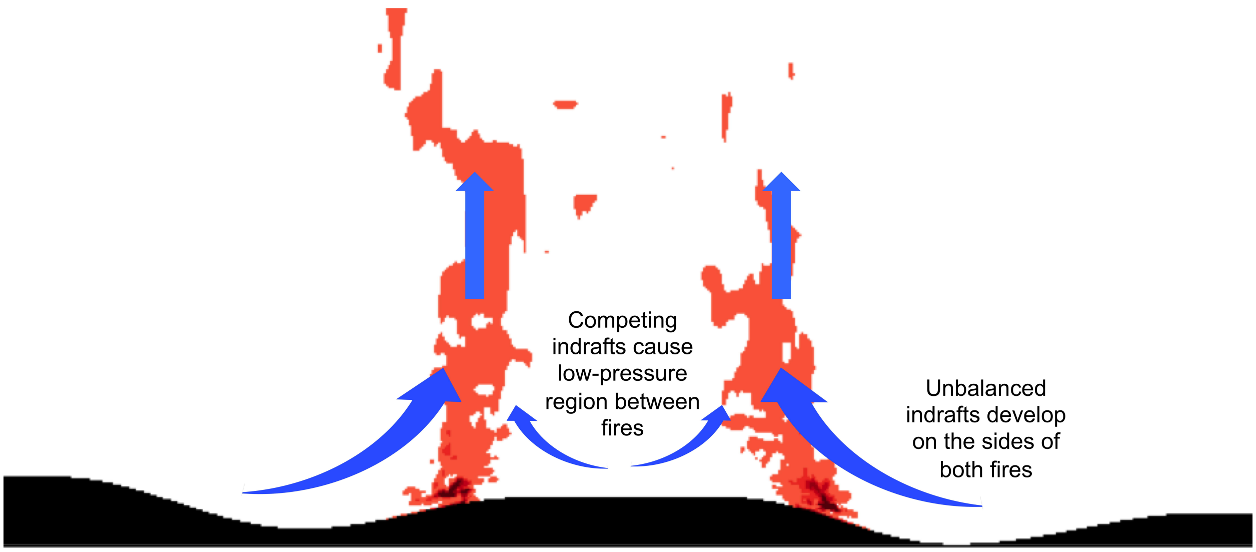

Cross-section of canyon topography

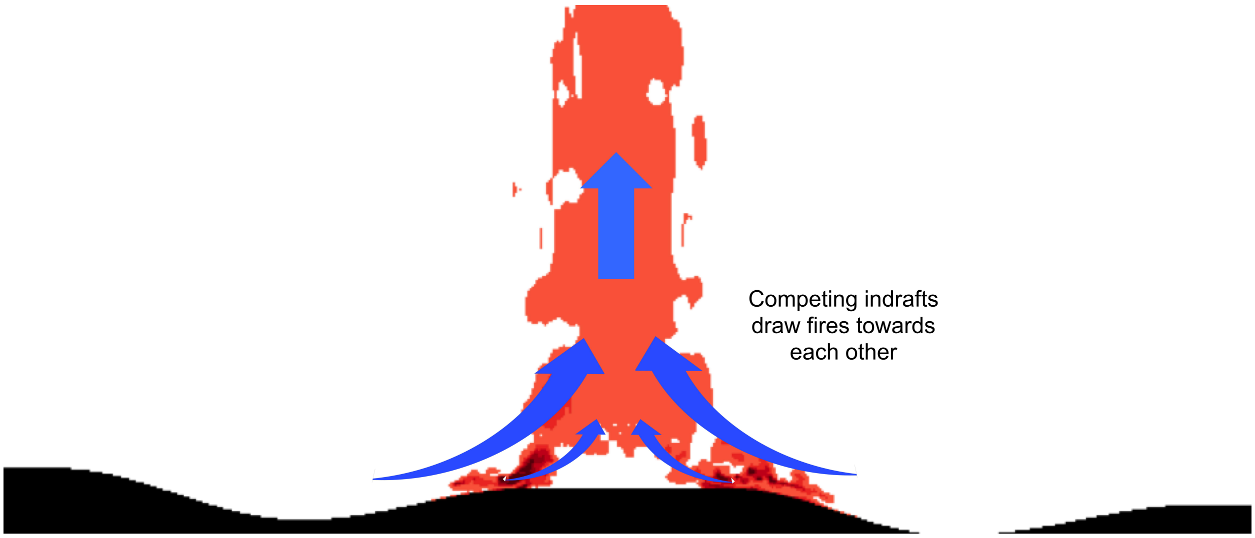

Figure 1. Cartoon of hypothetical concept of two fires on either side of a mesa, drawing each other over the mesa. In this case the ambient wind is thought to be parallel to the mesa and canyons (perpendicular to the image).

The details of what conditions constituted the "worst-case" scenario were not known even in the context of this hypothetical scenario. Thus a coupled fire/atmosphere behavior model, HIGRAD/FIRETEC, was used to refine the concept of the hypothetical scenario at TA-54. HIGRAD/FIRETEC, hereafter referred to as FIRETEC, consists of a macro-scale burning model integrated with an atmospheric fluid dynamics model, HIGRAD. HIGRAD is a fully-compressible atmospheric hydrodynamics model (Reisner *et al.* 2000) that was specifically designed to capture complex atmospheric phenomena involving high gradients of velocity or scalar quantities. HIGRAD had been applied to a wide range of atmospheric phenomena including: catastrophic space shuttle accidents and subsequent effluents, coupled wildfire/atmosphere behavior, urban fire and dispersion, coupled atmosphere/vegetation gas exchange, hurricane intensification, coupled turbine/wind interaction in wind energy contexts and explosive dispersion. Applications listed above are not well suited for traditional meso-scale atmospheric dynamics models due to the required grid resolutions, interaction between resolved solids and atmosphere or high gradients in temperatures, concentrations or velocities that are expected.

The portion of FIRETEC that represents the burning of material uses the solution of a coupled set of partial differential equations to represent the interaction between many of the critical physical phenomena that control fire behavior. FIRETEC simulates the interaction between the physical processes by explicitly resolving many of them through a finite volume numerical solution algorithm and stochastically representing fine-scale processes and heterogeneities that cannot be resolved in the numerical grid through subgrid models. FIRETEC was first applied to wildland fires and has been used to simulate historical fires (Bossert *et al.* 2000; Heller and Bradley 2002) and field experiments (Linn and Cunningham 2005; Linn *et al.* 2005; Linn *et al.*

2012a; Linn *et al.* 2012b). These previous modeling works have shown good agreement in comparison with observations. Various underlying physical phenomena have been individually scrutinized. For example, because FIRETEC was originally applied to wildland fires, its representation of flow through heterogeneous forest canopies has been shown to be realistic through comparison with the experiments of Shaw et al. (1988) and Raupach et al. (1987). A detailed description of the basic formulation and equation sets used in FIRETEC prior to its extension for urban fires is provided in Dupuy et al. (2011).

FIRETEC was developed for simulating fires on a landscape-scale (100s of meters to kilometers) where the details of the fuel configuration are seldom known. Due to the computational burden of simulating fires of in large domains and in light of the lack of fine scale knowledge of the fuels, the physics models that make up FIRETEC were intended to be used in a context where the fine (≤ meter) details of the combustion, flow and fuels are not resolved. Probability distribution functions and stochastic models are employed to represent these subgrid details and fluctuations of temperature and velocity. The simplified combustion model in FIRETEC assumes that resolutions are not sufficiently fine to represent individual fuel elements, flame sheets or nonlocal aspects of the combustion process. With the model assumptions in mind, the most appropriate resolutions for this model are between 1.5 m and 10 m. Going to finer resolutions begins to put some of the model assumptions and formulation in question. Although, FIRETEC has been applied to model wildland fires using several different resolutions, the majority of the validation work and comparison against field observations has been performed with horizontal resolution of 2 m. In order to take advantage of this previous work and comparison of model results against observations, the simulations performed in this report are all performed with 2 m horizontal resolution and 1.5 m vertical resolution near the ground (vertical resolution decreases with increasing height above the ground). Additionally, this resolution provides a good balance between resolution of physical processes and macroscale fuel arrangement against computational burden associated with higher resolution.

The topography surrounding TA-54 is considered known (Figure 2) and is not expected to change significantly in the next few decades from a wildfire perspective. However, in order to complete the specification of the hypothetical extreme fire scenario, fuel loads and distributions, wind conditions, and geometry of approaching fire must be formulated.

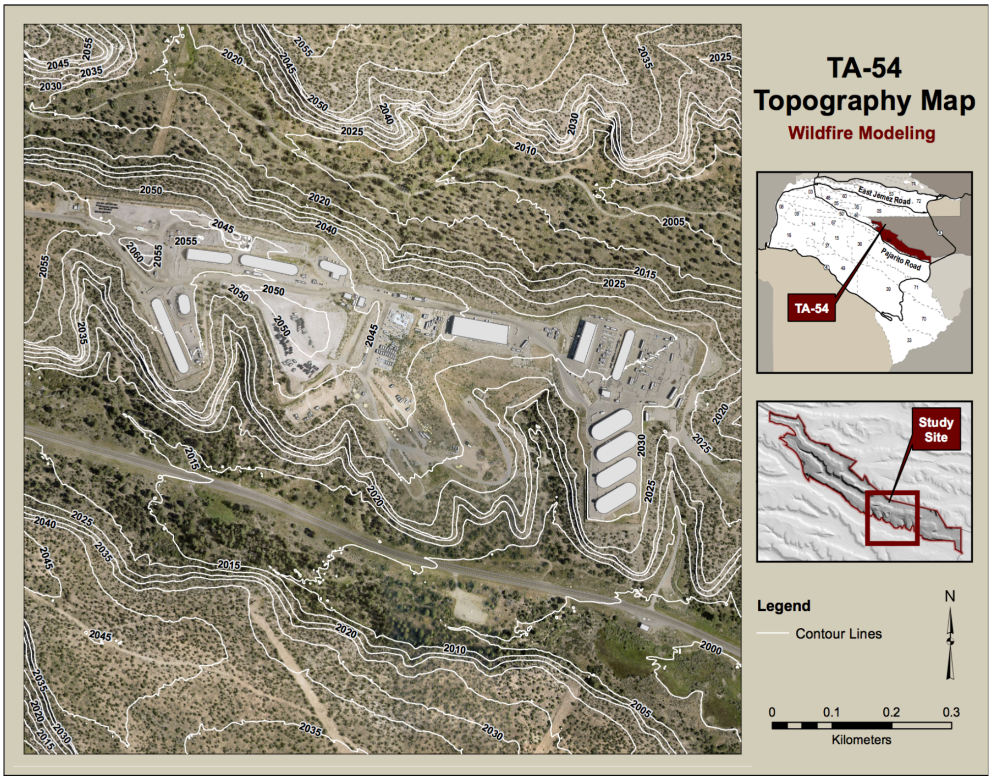

Figure 2. Topography surrounding TA-54

2.1 Fuels

The rough distribution of fuels surrounding the TA-54 was initially estimated based on a 2014 DRAFT LANL Landcover Map managed by EPC-ES recently in 2014 under the Long Term Strategy for Environmental Stewardship and Sustainability (LTSESS). Initial fuel classifications for the landcover map were derived by ISR-3 from WorldView 2 satellite imagery obtained in August of 2014, and training data based upon high-resolution aerial photography from Fall 2014 and plot data collected between March and September 2015. As there have been some fuels management and other disturbances in the area in recent years it was important to ground truth the fuels map through a site visit. David Keller (EPC-ES) provided site-specific expertise on the vegetation during the site visit and fuel types were adjusted and calibrated based on his consultation. The fuel type and loading derived from the site visit and original DRAFT LANL Landcover Map is shown in Figure 3.

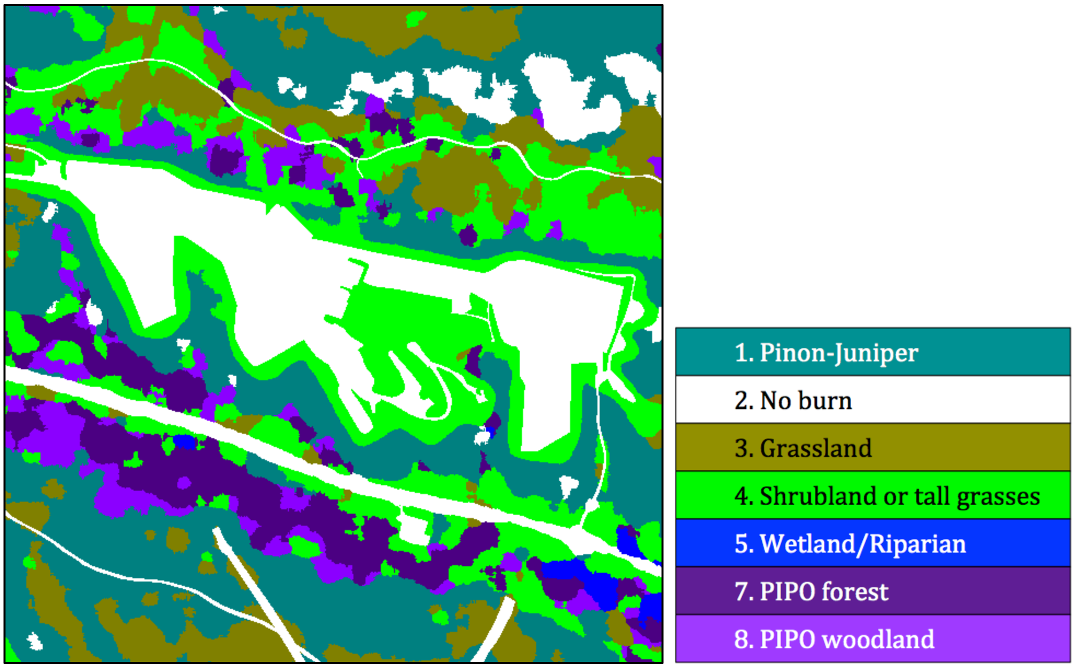

Figure 3. Fuels map for the area surrounding TA-54. The white region in the center of the domain represents parking lots, cleared areas or buildings, which are not easily ignited and were not allowed to burn in the simulations. In reality the nearest structure toTA-54-0375 is approximately 100 m away and even if it caught fire, it would not provide a significant heat flus TA-54-0375. In the simulation there was light fuel in TA-54-0375, representing debris and firebrands, in order to assure that we were modeling the worst-case scenario. In the legend PIPO stands for Ponderosa pine (*Pinus ponderosa*).

For these simulations, a focus was put on the fine fuels (foliage, grasses and twigs) since these are the fuels that have the fastest heat release per unit mass. There are minimal thick dry fuels (down logs, etc.) in the vicinity of TA-54 due to past fuel management efforts and live tree trunks are often not consumed in wildfires and certainly would not contribute to the rapid release of energy that would contribute to the convergence of two fire fronts. The loads distribution of fine fuels within the fuel type regions was accomplished by considering the reasonable ranges of loadings and vertical statures for each vegetation class and choosing fuel conditions that were considered to give the more extreme fire behavior. In the case of surface fuels, this meant choosing loadings and heights that were considered on the high side and initially discounting the fact that grasses in some areas were mowed. For example, the area just south of building 0375 has been mowed, but we used fuel loads more appropriate for taller grass. For the forest and woodland types, worst-case scenario meant using tree densities that did not reflect recent canopy thinning efforts or the drought-induced mortality that has reduced the density of living trees in this area. Although the canopy fuels have been thinned in recent years, tree densities were used from overly populated forests such as can be found in the Jemez Mountains or near Flagstaff, AZ. Using these tree densities, individual trees were located on the landscape using realistic distribution of crown heights and crown dimensions such as described in the research on Ponderosa pines (Linn *et al.* 2005) and on Pinon-Juniper (Linn *et al.* 2013). Fuel moistures were assumed to be 0.05 (mass of water/mass of dry fuel) in the surface fuels as that is reasonable during fire season. The canopy fuels were given fuel moistures of 1.0 as this is typical for live trees in this area even during fire season.

On the site of TA-54-0375, some combustible fuel load was permitted to remain on the ground. This fuel load of .58 kg/m^2 was used as part of an initial conservative estimate, as it is expected that there will be abundant firebrands landing in the area, which can be as large as big pieces of bark.

2.2 Wind speeds and pre-existing fire perimeter geometry

Unfortunately, it is not trivial to determine the worst-case wind scenario independently from the fire-perimeter geometry of an approaching fire. Therefore a series of idealized FIRETEC simulations were performed to identify worst-case combined wind and fire perimeter scenario. A simplified canyon-mesa-canyon topography for 1.2 km x 1.2 km area, shown in Figure 4, reflecting the nominal character of TA-54 without some of the more detailed site-specific side canyon features, was used for these simplified simulations.

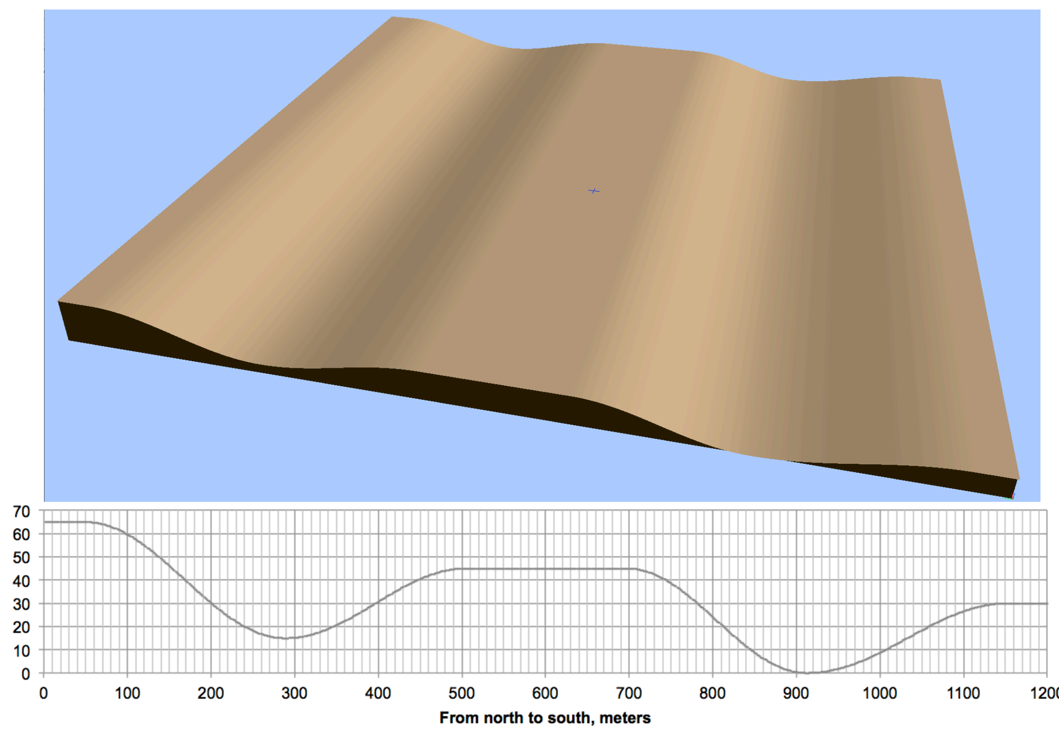

Figure 4. Illustration of simplified canyon-mesa-canyon topography used in wind speed/pre-existing fire perimeter geometry explorations in **(top)** 3-D visualization, with view from west (left is north) and in **(bottom)** 2-D elevation plot, from north to south.

In each of these idealized simulations, the ambient wind was assumed to blow parallel to the mesa and canyons. In this exploration/scoping series of calculations, three different nominal wind speeds, characterized by 1/7th power law boundary layer velocity profiles with 2, 6 and 12 m/s at a height of 10 m, were explored. Four different pre-existing fire-perimeter geometries, shown in Figure 5, (Canyon Bottom (CB), Canyon Bottom Mesa Top (CBMT), Parallel Lines (PL), U-Shaped perimeter (U)) were tested on simplified canyon-mesa-canyon topography. The Canyon Bottom (CB) fire perimeter geometry is intended to roughly approximate a scenario where two fires were previously making runs down canyon. This scenario is believed to have occurred at 3:00 am (local time) on June 27, 2011 on the Las Conchas fire based on satellite imagery. The hypothetical down canyon runs, which could have occurred due to density currents, can be pushed by winds that surge and lull. For this reason it is possible that the Canyon Bottom fire perimeter geometry shown in Figure 5 would have been formed during high winds but could be followed by periods of low, medium or high wind speeds. The Canyon Bottom Mesa Top (CBMT) geometry shown in Figure 5 connects the fires spreading down the two canyons with a fireline that spans over the top of the mesa. The potential for this perimeter geometry is also supported by satellite imagery from the Las Conchas fire. Simulations of fires proceeding from the CB and CBMT geometries illustrate that the two extended flanking portions of the fire in each canyon draw towards one another, limiting the expansion of the two fires out of the canyons. For this reason, it was postulated that if there were single lines of fire in both canyons approaching each other, the draw between them over the unforested mesa top would be greater. Thus the Parallel Lines geometry was examined as a scenario where two fire fronts were approaching from the two sides of the mesa. The final scenario, U-shaped geometry, is an extension of the two parallel lines with an additional line of fire connecting the two parallel lines and crossing over the mesa top.

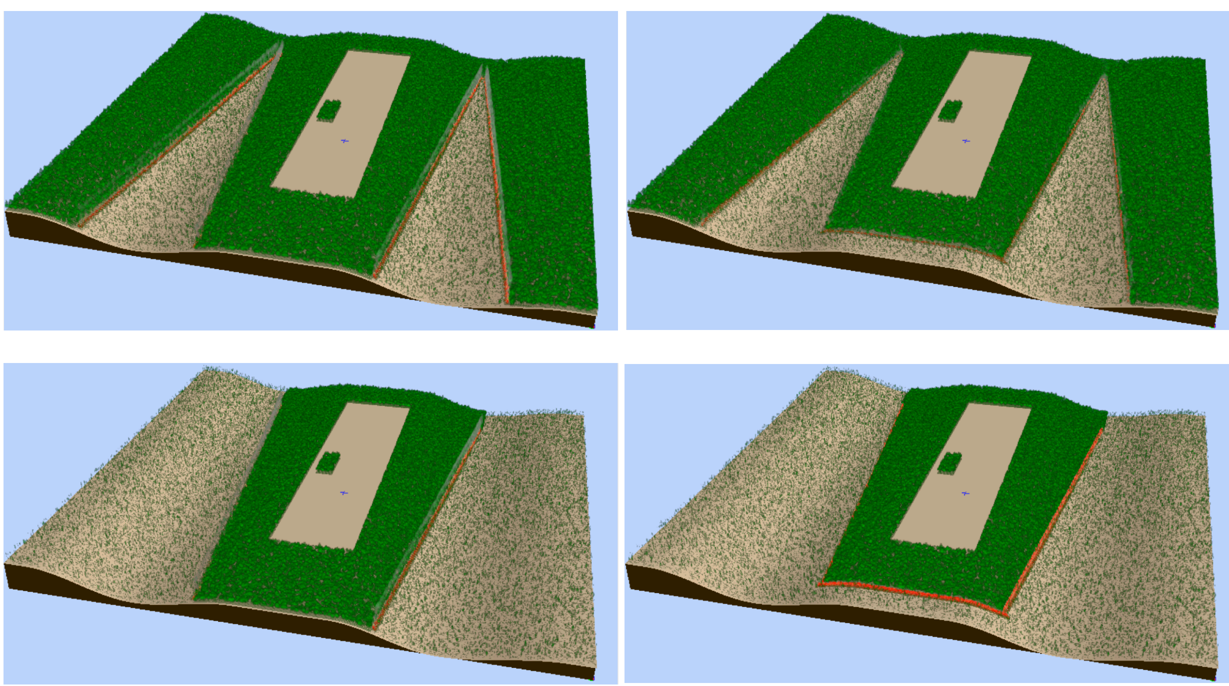

Figure 5. Illustration of four different ignition patterns used in wind speed/pre-existing fire perimeter geometry explorations: **(top left)** Canyon Bottom (CB) ignition; **(top right)** Canyon Bottom Mesa Top (CBMT) ignition; **(bottom left)** Parallel Lines (PL) ignition, **(bottom right)** U-Shaped perimeter (U) ignition

The fuel arrangement for these wind/preexisting-fire-perimeter-geometry explorations simulations was simplified much like the topography. The fuels in the canyons were specified as ponderosa pine and there was a clearing on top of the mesa. There were ponderosa trees upwind of the clearing just as exist at TA-54. One additional fuel feature that was added for illustration purposes was a patch of trees within the clearing at a representative location of building 0375 on the TA-54 mesa. This feature was used as a “diagnostic” that allowed rapid assessment of the severity of the convective and radiative fluxes at the location of concern (TA-54-0375). In addition, in each of the ignition scenarios described above, the vegetation “behind” the pre-existing lines was thinned such that 90% of the trees were removed and 80% of the surface fuels were removed as they would have been consumed by the fire as it achieved the “pre-existing” fire perimeters. The reason for going to the effort of removing these fuels is that their presence or absence impacts the airflow and entrainment rates, and as a result, the detailed natures of the fire behavior near the location of interest. The twelve wind/preexisting-fire-perimeter-geometry exploration simulations are summarized in Table 1 along with a graphical representation of their results.

Table 1. Summary of idealized simulations

Simulation	Wind Speed at z=10 m	Pre existing fire perimeter geometry	Results
CB_2	2 (m/s) (low)	Canyon Bottom	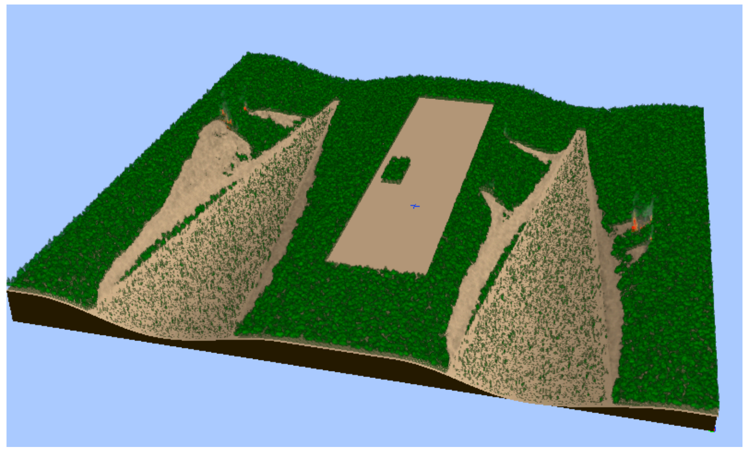
CB_6	6 (m/s) (mod)	Canyon Bottom	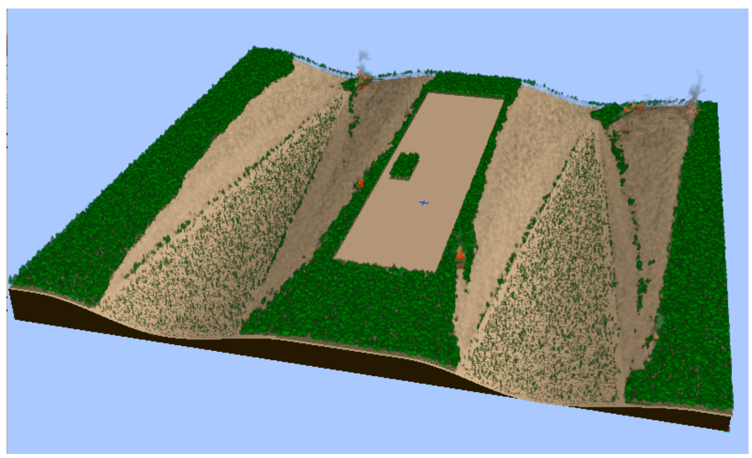
CB_12	12 (m/s) (high)	Canyon Bottom	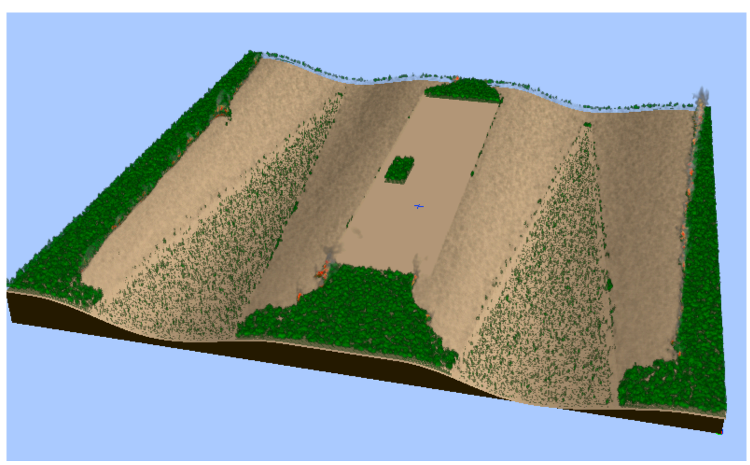

CBMT_2	2 (m/s) (low)	Canyon Bottom, Mesa Top	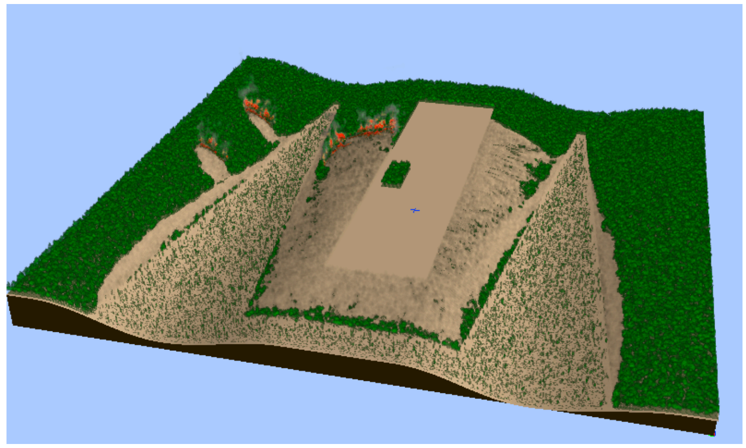
CBMT_6	6 (m/s) (mod)	Canyon Bottom Mesa Top	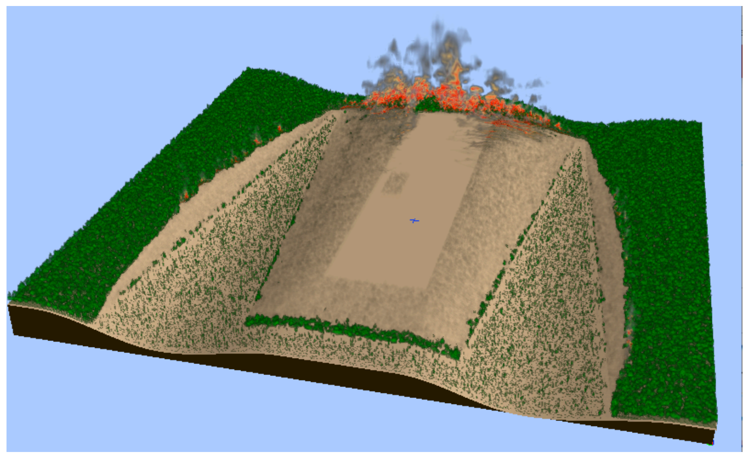
CBMT_12	12 (m/s) (high)	Canyon Bottom Mesa Top	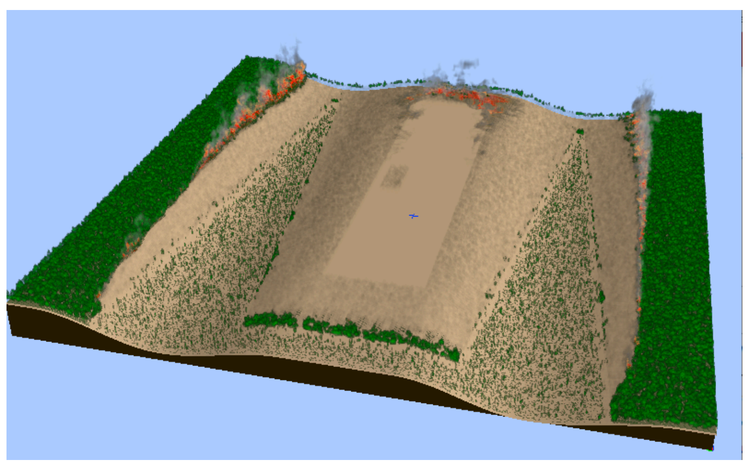

PL_2	2 (m/s) (low)	Parallel lines	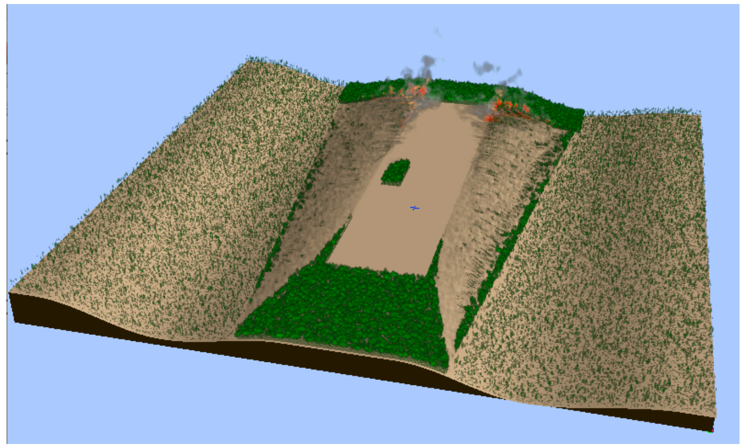
PL_6	6 (m/s) (mod)	Parallel lines	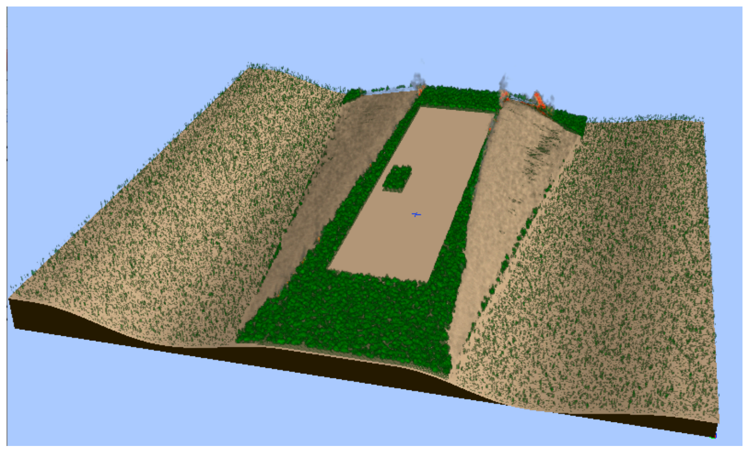
PL_12	12 (m/s) (high)	Parallel lines	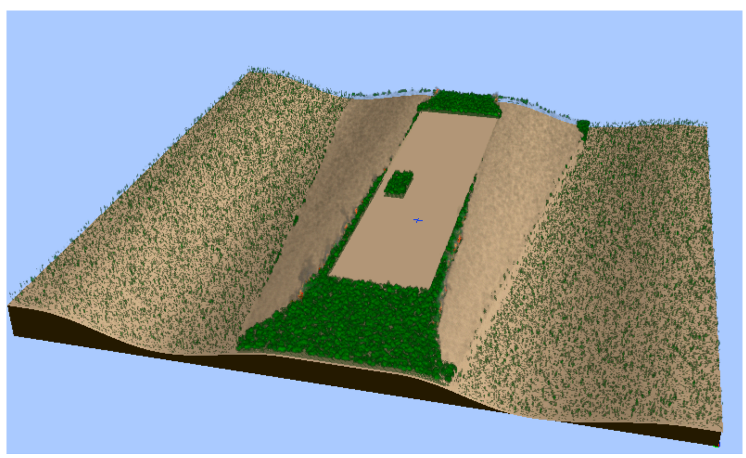

U_2	2 (m/s) (low)	U-shaped	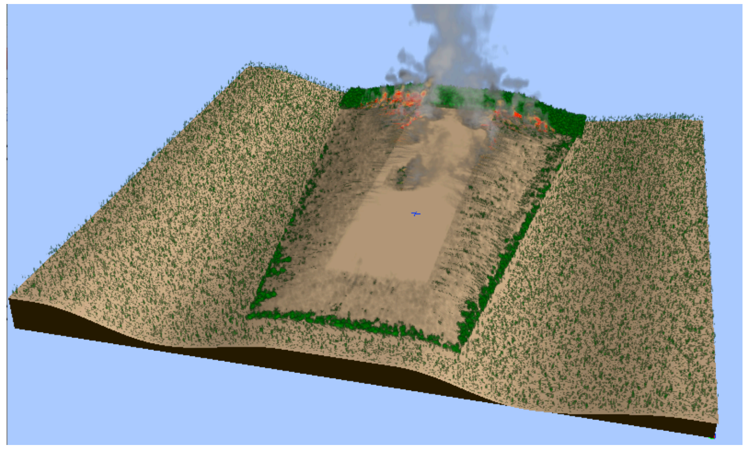
U_6	6 (m/s) (mod)	U-shaped	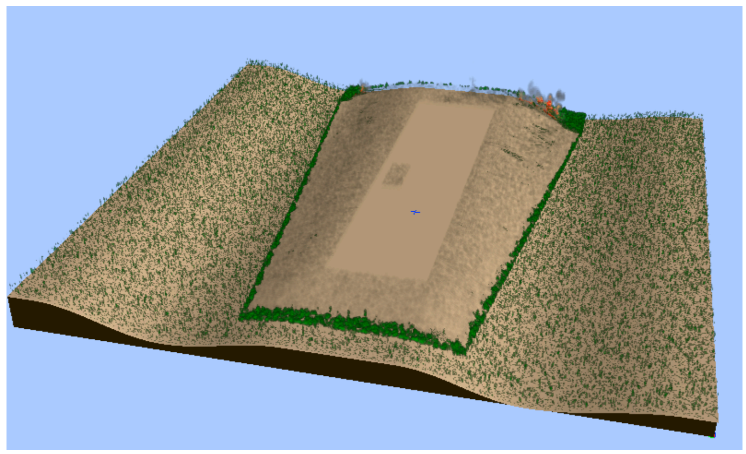
U_12	12 (m/s) (high)	U-shaped	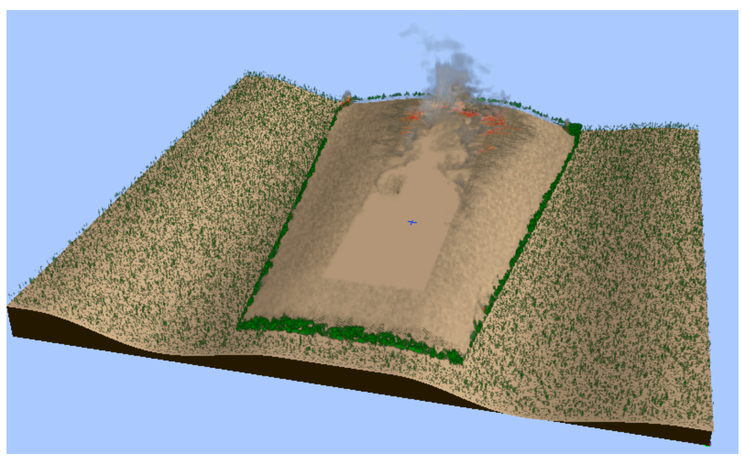

In the CB simulations, the results showed that with this pre-existing-fire perimeter the fire would only spread minimally under low-wind conditions, and spread with moderate vigor up the slopes on either side of the canyon at the higher wind speeds. In the moderate wind case, the lateral spread up the canyon sides is stopped before it consumes the vegetation just adjacent to the clearing. This stoppage of the lateral spread of the fire is likely due to the increased entrainment from the clearing, which is in a direction counter to the fire spread, and the decrease in slope of the topography as the fire approaches the clearing. None of the CB-simulation fires burned the trees in the small patch in the clearing.

In the CBMT simulations, the results showed that the presence of the fire on the upstream side of the clearing on top of the mesa has a significant influence on the fire behavior. In these simulations, the fires in the bottom of the canyon were able to burn up the hill slopes towards the mesa-top clearing under all ambient wind speeds and at moderate and high wind speeds the fires drew sufficient heat across the mesa to ignite and burn the trees in the small patch. The reason for this change in fire behavior compared to the CB simulations is a result of the upwind fire on the mesa top partially obstructing the mean wind flowing along the mesa top. This contributes to the low-pressure region that develops on top of the mesa. These effects increase the tendency for the fires in the canyons to draw towards each other.

In the PL simulations, the parallel lines of fire in the bottom of the canyons climb the hill towards the clearing on the mesa top under all wind speeds. However, under moderate- and high-wind speeds, the fires do not pull towards each other sufficiently to burn all of the vegetation on the edge of the clearing nor the patch of trees in the clearing. Under low-wind conditions, the fires pull together more strongly and burn a portion of the trees in the patch. This less-intuitive fire behavior trend of stronger fire behavior under low wind speed is a result of the reduction of the indraft interaction that occurs when strong winds are channeled down the mesa top. The fact that more vegetation on the edge of the clearing is burned towards the downwind side of the clearing indicates that the influence of the upwind mesa top winds decreases as you move downwind between the parallel fire lines. In other words, if the parallel firelines extended much farther upwind (longer fire lines) then the influence of the mesa top wind would be reduced and the convergence would be stronger.

In the U-shape simulations, the competition between multiple lines of fire in the canyon bottoms would be reduced just as with the PL cases and the wind blocking aspect of the fire on the mesa top will also be in effect as in the CBMT simulations. The result of these conditions is that the fires burned to the clearing and the patch of trees was burned at all wind speeds. The lateral spread and effect of converging fire fronts is increased due to the presence of the upwind fire on the mesa top, but the effect of this upwind fire diminishes when the upwind fire burns to the clearing and disappears when it has no more fuel to burn. The impact of the upwind fire is also a function of the length of the canyon firelines and the wind speed along the mesa top. The effects of the U-shaped geometry is highest in the low wind speed case where the upwind mesa-top fire is moving slower, less air penetrates through the plume and the fire runs out of fuel (due to the clearing) at a later time.

Based on these simulations, the worst-case geometry for “defining” the pre-existing-fire perimeter is the U-shaped perimeter. This scenario is somewhat contrived but does capture some of the features that were exhibited by segments of the Las Conchas fire perimeter. The artificial nature or difficulty to achieve this pre-existing fire perimeter is not considered for the purpose of this exercise, as the objective is to identify any possible wildfire risk to the Perma-Con in building TA-54-0375. It should be acknowledged that a potentially more dangerous fire geometry was not considered, due to the unlikely possibility that it would occur naturally. This scenario would be one where the fire forms a circle around TA-54 starting around 100 m from the clearing in all directions with minimal wind. This ring fire scenario would be extremely dangerous, but is not expected in nature.

3. Converging fire simulations for TA-54

The topography, fuels, wind speeds, and pre-existing fire geometry described above were used for the specification of the initial and boundary conditions of fire simulations of converging fires TA-54. The fuels, being specified by combination of landcover map, site visit and conservative estimates of fuel loadings and vertical distribution, were combined with real topography and a U-shaped fire perimeter shown in Figure 6.

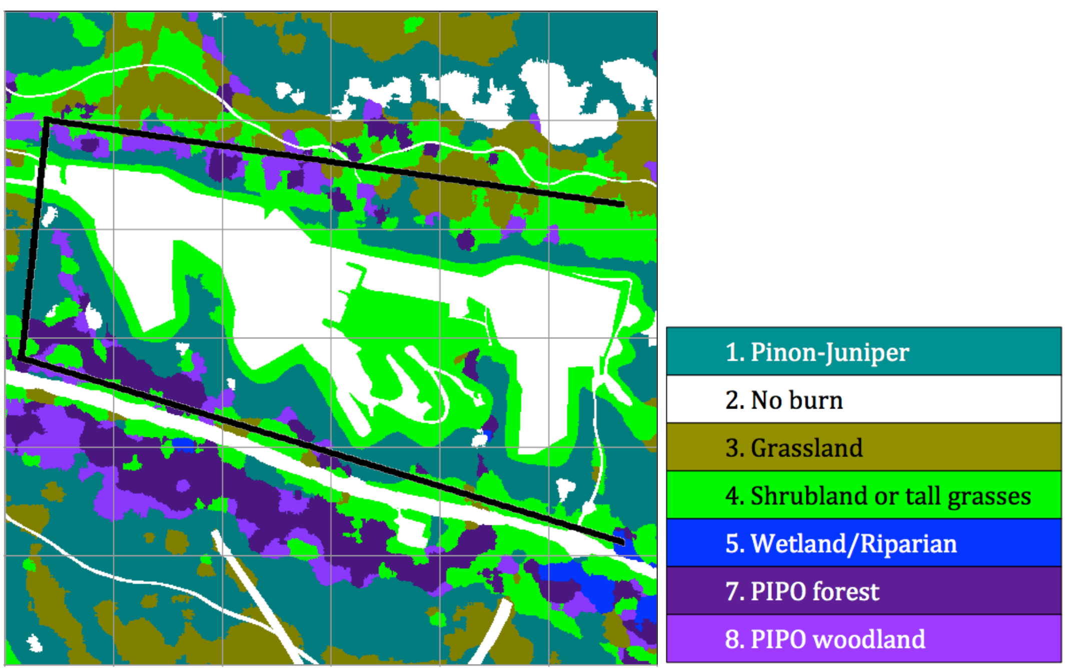

Figure 6. Landcover/fuels map of TA-54 showing fire perimeter at the beginning of simulations (black lines).

A light ambient wind (2 m/s) was angled parallel to the general direction of the mesa top as in the idealized simulations above, in order to investigate the scenarios similar to Las Conchas fire, which were shown in idealized simulations to have potential of fire risk even in the case of low wind condition (U_2).

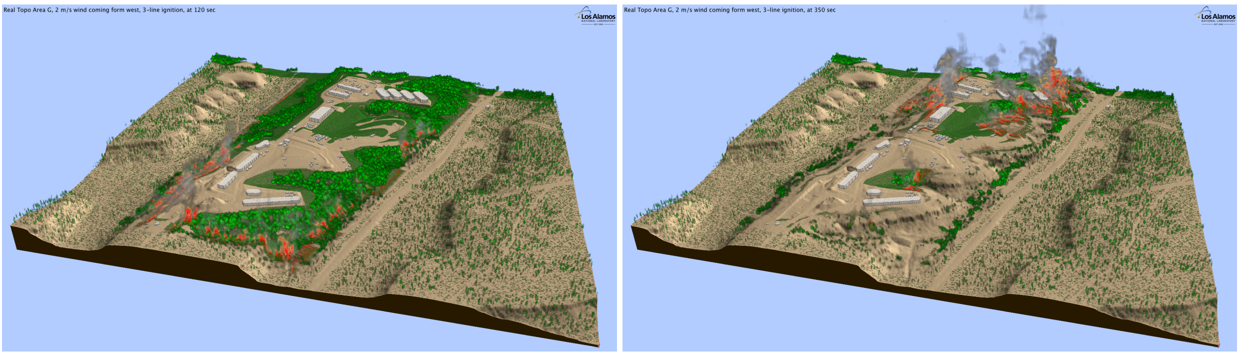

Figure 7. Visualization of U-shaped fire perimeter simulation of TA-54. **(left)** 120 seconds after ignition, **(right)** 350 seconds after ignition.

This simulation (Figure 7) with U-shaped pre-existing-fire perimeters showed convergence of the fires on the north and south sides of the mesa and heat was drawn over the area where dome 0375 is located. The buildings are shown in the graphics, but they are not actually present in the simulation, under the assumption that the fabrics of outer building walls were already melted. The low-wind simulation resulted in the largest radiative heat fluxes in the vicinity of the Perma-Con.

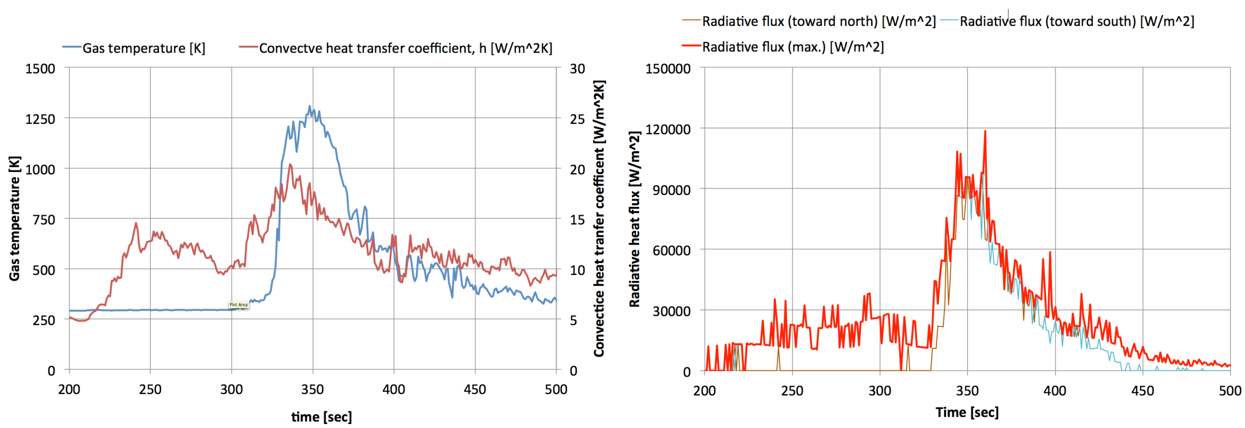

Figure 8. Thermal environment from U-shaped fire perimeter ignitions of dome TA-54-0375: **(left)** gas temperature and convective heat transfer coefficient over 300 seconds, **(right)** radiative heat flux over 300 seconds.

The conditions that the Perma-con was exposed to are shown in Figure 8. In Figure 8, the potential for convective heat transfer is described in terms of the maximum gas temperatures and local maximum convective heat transfer coefficient in 2 m x ~1.5 m elements of an imaginary (virtual) sensor plane that was 82 m long and 16 m high in the central portion of the dome. This coefficient is an estimate based on conventional heat transfer coefficient formulations for flow over a flat surface with ~15 m dimensions (Incropera and DeWitt 2002). This estimate for the heat transfer coefficient is based on local maximum wind speed and air densities, but does not include the effects of the Perma-Con structure on the wind field. This is considered a conservative approach for the most part since the Perma-Con will block the winds and slow them down in most places, thus reducing the flux to the Perma-Con. It is acknowledged that this does ignore the potential of trapped hot gases on the downwind side (in the wake) of the Perma-Con. If there were significant combustibles surrounding the Perma-Con, this could be the location of maximum fire intensity, but there are assumed to be only minimal debris in this area (consistent with combustible loading criteria for these facilities). For the purpose of prescribing the conservative boundary conditions for a detailed Perma-Con heat transfer simulation that would include the contents of the Perma-Con, the maximum gas temperatures can be paired with this heat transfer coefficient even though the temperatures will vary from point to point on the surface and actually drop as heat is transferred to the Perma-Con. The maximum temperature and heat transfer coefficients were then assumed to exist over the entire surface of the Perma-Con in order to assume a conservative estimate of the heat transfer. Figure 8 also shows the radiative heat flux from the north and from the south sides of the Perma-Con. These fluxes are intended to be conservative estimates of the incident radiation flux on the Perma-Con and are not expected to be representative of the average radiative flux. The detailed locations of the hottest portions of modeled fire are not expected to be exactly in the same as a real fire, given the heterogeneous nature of the fire behavior. Thus in order to assure conservative estimates as the worst case scenario, radiative fluxes was extracted from the model results as the maximum local flux passing through and 2 m x ~1.5 m element of an virtual sensor plane that was 82 m long and 16 m high in the central portion of the dome, just as done for the convective environment described above. Through this methodology, we eliminate the dependence of the results on the details of the local heterogeneity of the fire and heat fluxes at the approximate location of the Perma-Con, which would depend on details of a real scenario that are impossible to predict for the simulation. The maximum of the north and south radiative flux at any given point in time (shown in red) is suggested for the conservative boundary conditions for a detailed Perma-Con heat transfer calculation. For a conservative estimate, it may be reasonable to use an emissivity of 1 for the Perma-Con during the period of high radiative heat flux, since it could be covered in black soot by the time the heat flux is a maximum.

The heat transfer environment suggests that the majority of the heat transfer from the fire to the surface of the Perma-Con is likely in the form of radiative heat transfer. Even though the convective heat flux cannot be computed explicitly without knowing the temperature of the Perma-Con surface, the convective heat flux is estimated to be less than 20,000 W/m^2 (if there is 1000K temperature differences between gas and Perma-Con) compared with the 120,000 W/m^2 provided by the radiation flux to the surface. This value was less than peak values measured from some crown fires, such as 189,000 W/m^2 and 300,000 W/m^2 as in the Mill Creek and Rat Creek fires respectively (Frankman *et al.* 2013). Additional comparisons can be found in the thesis of Frankman, *Radiation and Convection Heat Transfer in Wildland Fire Environments* (2009), in which different fuels and the measured radiative fluxes are discussed. As examples, ground, brush, and crown fire peak radiant fluxes were measured, with values as low as 18,500 W/m^2 for ground fires, 120,000 W/m^2 for brush fires, and crown fires as high as 300,000 W/m^2. However, the fuel (vegetation) load consumed in these crown fires in the vicinity of the sensors on the order of between 3 kg/m^2 and 5 kg/m^2 compared to the 0.58 kg/m^2 to 1.46 kg/m^2 for the debris and shrubs in the vicinity of the Perma-Con in this simulation. A portion of the Rombo fire (Frankman *et al.* 2013), which was a brush fire, was reported to have peak radiative flux of 130,000 W/m^2 while consuming only 0.54 kg/m^2, but this fire was burning on a steep slope. This makes the fire a reasonable analogue as the multiple-fire indraft-induced convergence of the plumes could tend to hold the flames and hot gases closer to the surface, which can also occur in steep slope fires. The duration of the significant heat transfer is around 200 seconds but the high heat flux (>60,000 W/m^2) in these results is on the order of a half a minute. These time scales from the simulations are of the same order of magnitude as the resonance time scales of fine (flashy) wildland fuels and similar to the timescales for the high temperatures of the crown and brush fires from measurements of actual fires described above. However, the duration of these heat fluxes is tied to the length of time when the indraft strength is strong enough to pull the hot gases through the area where building 0375 was located. This depends on the duration the very high heat release rates from fuels nearest to the 0375 site. As the heat release rates diminish the plumes will stand more vertically (away from building 0375) and as the fuels upwind on the mesa burn out the ambient winds will further reduce the draw between the two north and south fires. These simulations indicate that if this drawing phenomenon were to occur it would likely be relatively short in duration (<100s of seconds) with these fuel loads and topography.

Careful study of the dynamics of the fire approaching from the north and south canyons showed that the fire in the north canyon arrived at the edge of the mesa top clearing sooner than the fire line approaching from the south. In order for the concept of the converging lines to produce maximum heating of the Perma-Con, the fires should converge on the site at the same time. Building 0375 is not centered on the mesa and is closer to the fire line approaching from the North. Thus it should not be unexpected for the fire coming from the North to arrive at 0375 first. In order to further refine the "worst case" an additional simulation, referred to as the "4-line" simulation was performed in which a spur ignition line was introduced in one of the side canyons. This could potentially occur due to spot fire ignitions from embers that were drawn into the side canyon by the converging winds. The ignition for this simulation is illustrated in Figure 9.

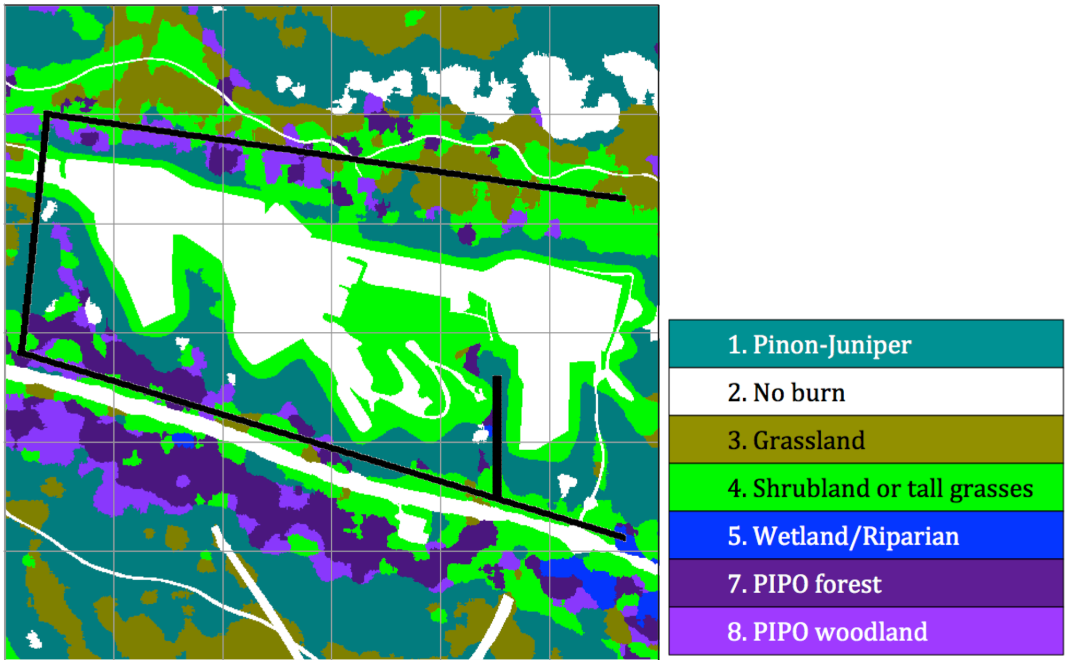

Figure 9. Illustration of additional "spur" ignition added to TA-54 U-shaped pre-existing fire perimeter

The results of adding the spur ignition line is that the fires, illustrated in Figure 9, converge on building 0375 at closer times than without it as shown in Figure 10, and the resulting heat in the area of the Perma-Con is increased. The estimated heat transfer environment for the Perma-Con is summarized in Figure 11, which shows on the order of a 150% increase in peak radiative heat flux although the duration of the high heat flux rates was similar in magnitude. The heat fluxes in this simulation exceed those of the Rombo brush fire on steep slope but in the simulation the converging fire fronts further limit the extent to which the flames and hot gases can stand up.

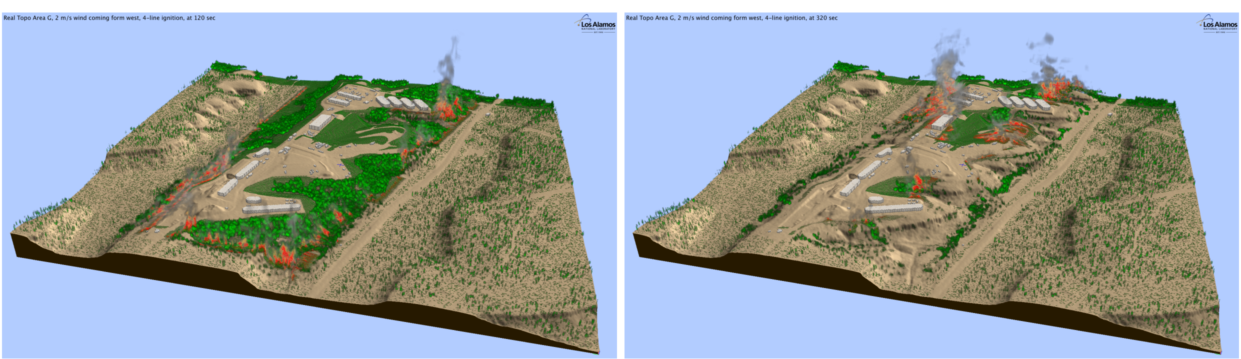

Figure 10. Visualization of U-shaped fire perimeter plus spotfire ignitions in side canyon to the south of dome TA-54-0375 simulation (4-line simulation) of TA-54. **(left)** 120 seconds after ignition, **(right)** 320 seconds after ignition.

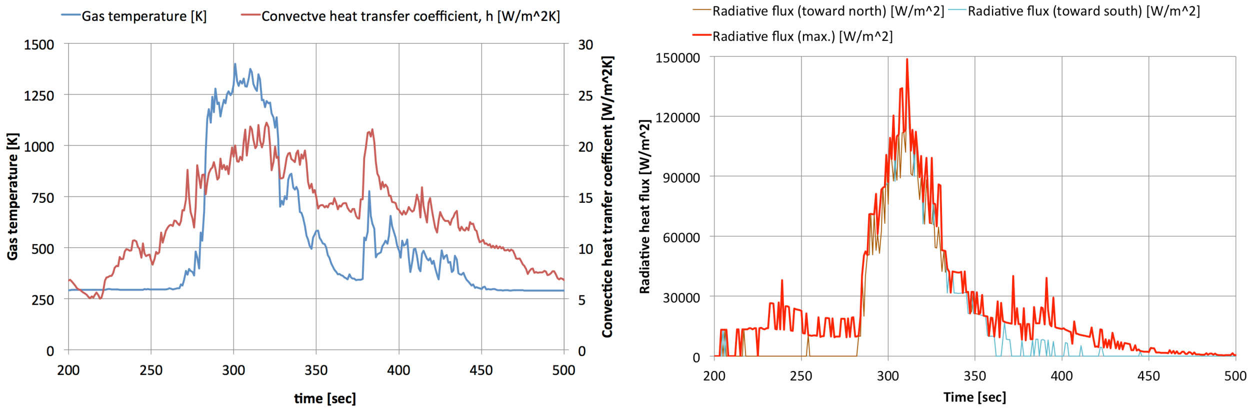

Figure 11. Thermal environment from U-shaped fire perimeter plus spotfire ignitions in side canyon to the south of dome TA-54-0375 (4-line simulation): **(left)** gas temperature and convective heat transfer coefficient over 300 seconds, **(right)** radiative heat flux over 300 seconds.

4. Additional Scenario

Through the course of performing the fire simulations of the real TA-54 site, an additional scenario was deemed worth consideration as a possible worst-case scenario. More specifically, this scenario is a long fireline in the canyon to the north of TA-54 driven by a strong wind (10 m/s) from the Northwest. This is also a plausible wind direction. The worst case would be for this fireline to be continuous in the bottom of the canyon and not have significant breaks in it. This is because long fire lines tend to spread faster and more intensely then short or broken firelines. Achieving this long fireline would likely require complicated shifts in wind direction and magnitude, but as with the analysis above, the likelihood of getting this pre-existing fire perimeter is not the focus of this exploration.

This simulation, which is illustrated in Figure 12, produce a thermal environment for the Perma-Con, summarized in Figure 13, in which heat fluxes were comparable in magnitude to the U-shaped scenario described above, but the duration was slightly longer.

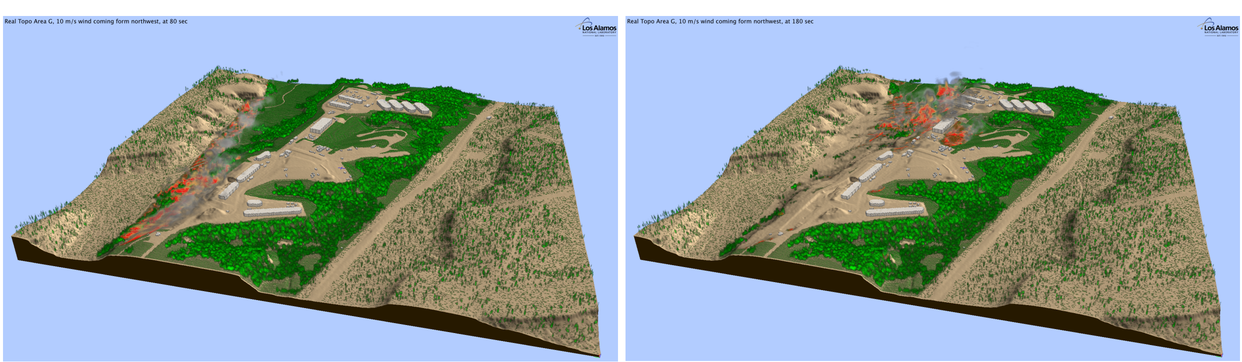

Figure 12. Simulation results from TA-54 fire simulations with long fire line in the canyon to the north of the TA-54 mesa and a 10 m/s wind from the Northwest. **(left)** 80 seconds after ignition, **(right)** 180 seconds after ignition.

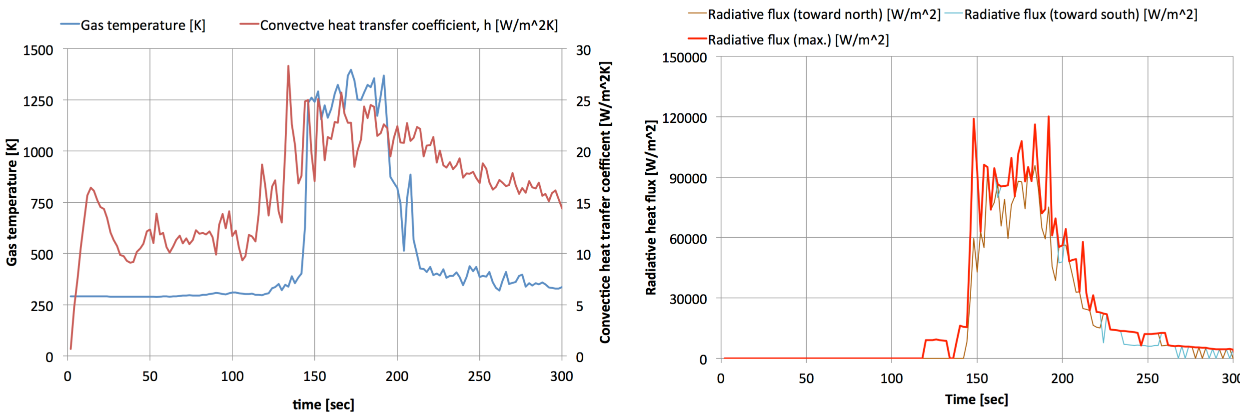

Figure 13. Thermal environment induced by long fireline driven by Northwest wind: **(left)** gas temperature and convective heat transfer coefficient over 300 seconds, **(right)** radiative heat flux over 300 seconds.

5. Mitigation Efforts

Based on more detailed calculations of the heat transfer in the Perma-Con, which are described in a companion report, the thermal environment produced by the U-shaped fire perimeter with spotfire ignitions in side canyon to the south of dome TA-54-0375 exceeded the levels that risk mitigation experts were willing to accept. In this scenario, referred to as the 4-line simulation, the combination of 0.58 kg/m^2 debris loading inside the dome perimeter and the tall grass/ shrub fuel loading, 1.46 kg/m^2 in the vegetated areas closest to the dome on the north and south sides were contributing significantly to the escalation of this thermal environment. The 4-line simulation had been used to estimate the worst-case scenario, but it was felt that the debris loading inside the dome perimeter was unrealistically high and that a more realistic (but still conservative) debris loading (0.058 kg/m^2) should be used inside the dome perimeter. Additionally, cost effective fire-mitigation efforts, periodic mowing/raking the grasses and shrubs nearest the Perma-Con to reduce their height from 0.7 m tall to 0.07 m tall (thus, fuel loading from 1.46 kg/m^2 to 0.146 kg/m^2) should be scheduled regularly during fire seasons.

With this reduction in debris loading in the Perma-Con and the fuels-mitigation efforts near the Perma-Con, an additional simulation was performed with the 2 m/s ambient winds. For the first of the simulation with the mitigated loads, all of the other simulation parameters were the same as in the 4-line simulation. This simulation showed a significant reduction in convective and radiative heat flux to the Perma-Con surfaces, as shown in Figure 14. However, the discontinuous nature of the radiative flux plots indicated that the Monte Carlo-based estimate of the radiation to the Perma-Con was under resolved for this scenario, in which the distance between the fire (radiation source) and the virtual sensor plane is far greater than the previous simulations.

When the fuels in the 0375 dome were set to 0.058 kg/m^2 and the grasses/shrubs were mowed, there are significantly larger distances between the intense fires on the north or south sides of dome 0375 and the Perma-Con (or virtual target plane for the radiation fluxes) than in the unmanaged fuel simulations, such as the 4-line simulation. This larger distance is a key factor in reducing the heat flux to the Perma-Con, but is also has implications for the accuracy of the Monte-Carlo-based (MC) radiation flux calculations. This is because not only does the radiation density start to fall off with the square of the distance from the source for larger distances (large compared to the size of the radiation source) but also does the density of MC rays. Thus the spatial distribution of the MC-based radiation flux becomes artificially more heterogeneous as the distances get too large. This modeling deficiency is illustrated by the unphysical discontinuous and stair-step nature of the red curve in Figure 14 or grey curve in Figure 15. This high points of this stair-step pattern in the plot of the maximum flux through the virtual plane is expected to be an overestimation of the flux as the under-resolved MC ray distribution leads to peak fluxes that are much higher than the real fluxes. There are also places on the virtual plane that will have much lower than realistic fluxes, but they are ignored due to the fact that we are taking the maximum local fluxes to the plane as our conservative estimate of the radiative flux to the whole Perma-Con.

For a first conservative estimate of the fluxes to the Perma-Con under the mitigated fuel conditions, a smoothed curve (red curve in figure 15) was fit to peaks of the maximum radiation fluxes. This is acknowledged as having significant inaccuracies, but is expected to result in fluxes that are much higher than the real fluxes to the Perma-Con. In order to estimate the potential safety factor that is built into this smoothed curve fit estimate of the fluxes, a series of refined MC simulations were performed. Figure 15 illustrates the impact of increasing the number of rays that are emitted in between MC convergence tests as well as tightening the convergence threshold, which is compared to the normalized difference in the absorbed fluxes as more rays are emitted. The series of simulations shows relative convergence in the radiative fluxes with higher fidelity MC calculations. The higher fidelity MC calculations show much lower maximum radiative fluxes to the virtual plane then estimated by the smoothed flux curve as well as the standard MC simulations. The convergence provides confidence in the maximum flux values obtained by the higher fidelity MC calculations and theses are the fluxes delivered for the detailed Perma-Con heat transfer calculations. The smoothed red curve was provided as a means of checking the sensitivity of the Perma-Con heat transfer calculations to the radiative fluxes computed by FIRETEC.

These refined MC simulations resulted in peak radiation fluxes that were approximately 1/20 th of the 4-line simulation fluxes before the mitigation of the fuels and reduction of the debris inside the dome perimeter. The thin black, red, green, purple, orange or blue curves in Figure 15 illustrate the use of successively refined (through increases in the number of MC rays in a batch and tighter flux convergence test criteria) calculations to demonstrate convergence. The radiative flux estimates from these refined calculations illustrated a significant influence of removal of fuels in the near vicinity of the Perma-Con and dropped the predicted radiative fluxes below even those typically measured in grass or surface fires (Frankman *et al.* 2013). This is not unexpected as these surface fuel loads are lower than those of grass fires, but still conservatively represent the fuels expected at .146 kg/m^2 associated with mowed grass and shrubs. These refined MC calculations were provided for the detailed Perma-Con heat transfer calculations. A smoothed curve fit version of the under-resolved MC calculation (red curve in Figure 15) was provided as a means of evaluating the sensitivity of the detailed Perma-Con heat transfer calculations to uncertainty in the FIRETEC simulations.

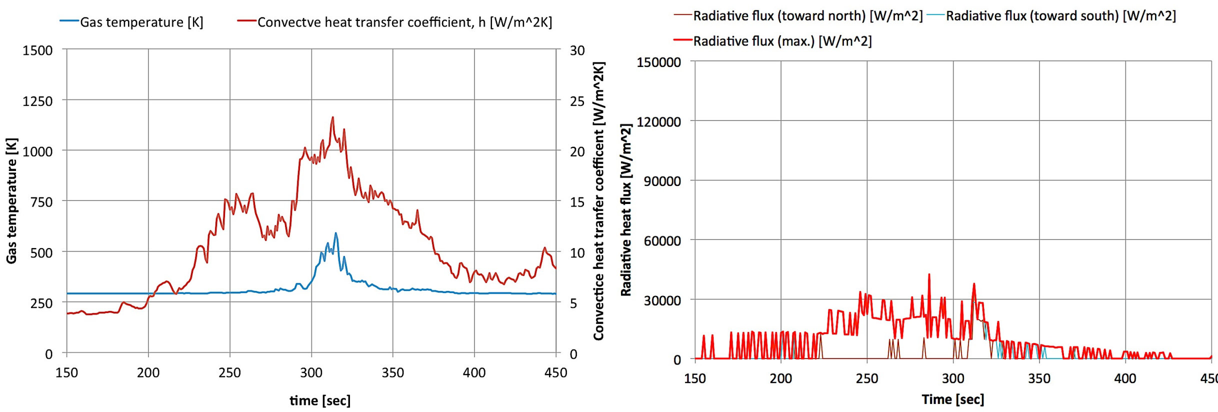

Figure 14. Thermal environment induced with 4-line fire perimeter and mitigated fuel loads near TA-54-0375: **(left)** gas temperature and convective heat transfer coefficient over 300 seconds, **(right)** radiative heat flux over 300 seconds.

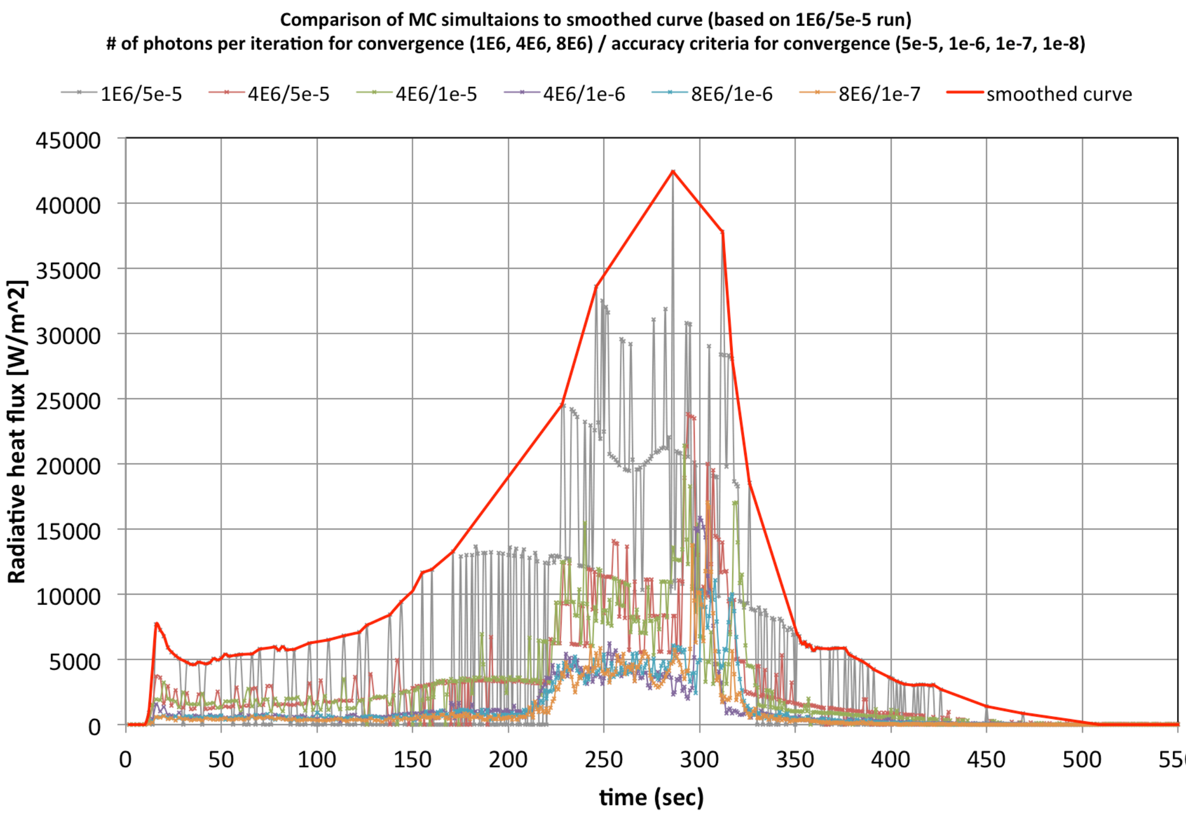

Figure 15. Maximum radiative fluxes to plane in a series of simulations with successively refined Monte Carlo calculations. The numbers of MC rays emitted in between convergence tests (left number in the legend labels) were increased and the convergence criteria (right number in the legend labels) were decreased. The orange, purple and blue curves show relative convergence to radiative fluxes well below the values estimated when the MC radiation was under resolved.

6. Sensitivity Analysis

The fuel loads that were used were considered conservative due to the fact that we used realistic tree density values for 1) unthinned forests, 2) higher grass loadings than would be expected for tall grass, and 3) an estimate for the combustible thermally thin debris in the dome 0375 perimeter that was appropriate for 29 firebrands/m^2 based on typical 2 g size, which is modeled after real firebrands, ~50mm in width or diameter with ~5mm in thickness, found after the Oakland Hills Fire in 1991. In order to determine the potential impacts of the conservative nature of these values on the thermal environment surrounding the Perma-Con, we performed an additional calculation as a sensitivity analysis. We reduced all of the fuels by 20% from those used in the simulations with mowed grass and then performed the calculation again. We did not use higher fuel loads than previously used because the original set of simulations was already determined to be a conservative worst-case scenario in terms of fuel load.

The radiative flux from the new 80% calculation is plotted in Figure 1. By comparing the simulation with the full conservative loading (labeled 100% in figure 1) and the simulation with all fuels reduced by 20% (labeled 80%), it is apparent that the net radiative heat flux to the Perma-Con is a nonlinear function of the fuel load and by being conservative with the fuel loads we have achieved and even more conservative estimate of the heat flux to the Perma-Con. This non-linearity occurs due to the fact that the intensity of the fire, which depends heavily on the fuel load, determines the convergence of the plume above the mesa and building 0375. As the fuel loads decrease, not only is there less heat being emitted, but also the trajectory of the hot gases is less conducive to heat fluxes to the Perma-Con due to the plumes converging to a lesser degree over the mesa top.

Given the degree of forest thinning that has actually occurred in the area, we also view the 80% fuel loads used in this sensitivity analysis to be conservative. Based on the sensitivity analysis calculations, the radiative flux values used in the Perma-Con analysis were higher than the fluxes from the 80% calculation by a factor of about 1.7 for the cumulative flux and nearly a factor of 3 for the peak flux. Based on the fact that we feel that the 80% simulation was still conservative, we can therefore conservatively estimate the safety factor for the fluxes to the Perma-Con at least 1.7 based on the sensitivity analysis. Additionally, the heat fluxes used for the entire Perma-Con boundary conditions were the maximum heat fluxes over a virtual sensor plane that was 82 m long and 16 m high. This adds additional conservatism due to the fact that in reality the fluxes to all sides of the Perma-Con will not be at this peak value and will actually be significantly lower. It is difficult to determine an the exact additional contribution to the factor of safety (above the 1.7) due to the fact that this deviation from the peak flux on the virtual sensor plane to the average flux over the surface area of the Perma-Con changes with time.

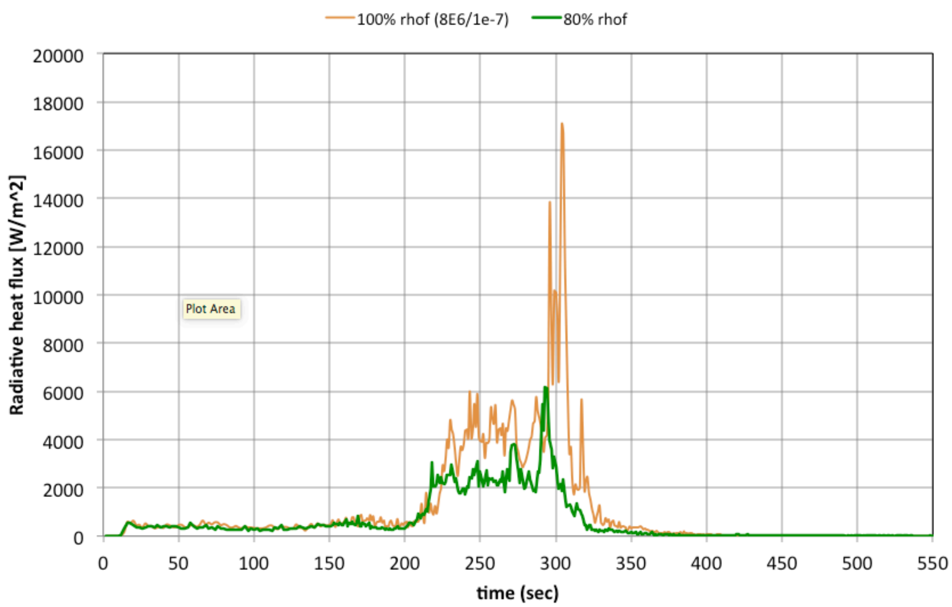

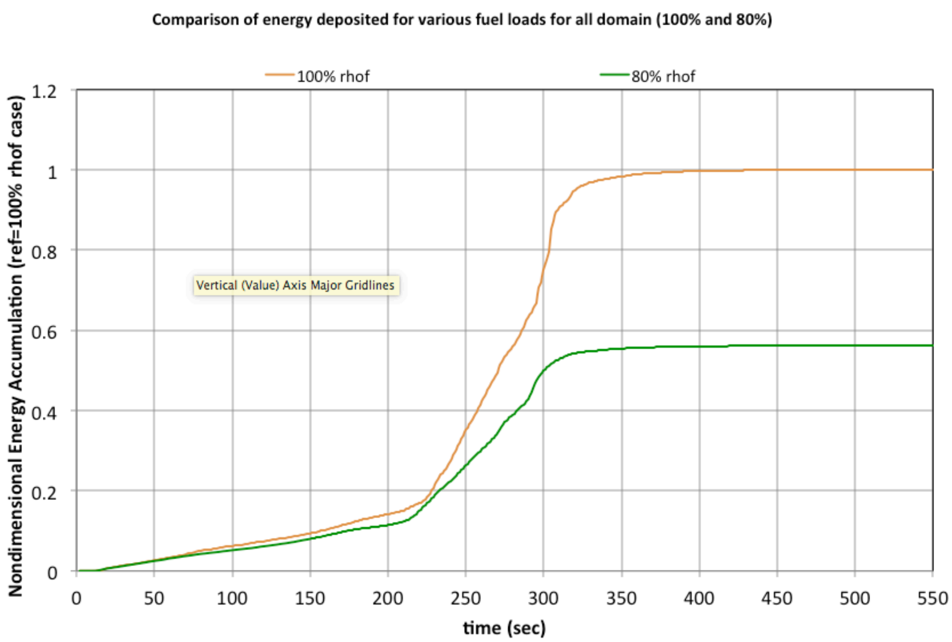

Figure 16. Thermal environment near TA-54-0375 induced with 4-line fire perimeter and mitigated fuel loads (yellow) and fuel loads reduced to 80% of mitigated loads (green) near TA-54-0375: **(top)**, and accumulation of deposited energy as a function of time **(bottom)**.

7. Conclusions

A previous fire risk evaluation determined that the risk of fire spreading over building TA-54-0375 and posing significant risk to the contents of this building were low based on probable fire behavior. This was mainly due to the lack of combustible material on the TA-54 mesa top in the vicinity of building 0375. In an effort to identify any possible natural wildfire threat to the contents of a Perma-Con container in LANL's building TA-54-0375, LANL risk management authorities and fire behavior experts realized that, based on Las Conchas fire perimeter data, there was a remote chance of fires occurring in the canyons on both sides of TA-54. If this were to occur, the two fires could hypothetically interact to draw fire and hot gases over the mesa top and significantly increase the heat flux to the Perma-Con.

A series of simplified scoping-type simulations were used to explore the possibility of two fires interacting in this way over the relevant distances. This scoping study included 12 exploratory simulations with three wind speeds (low, moderate, and high) and four different pre-existing fire perimeter geometries. The simulation results illustrated that there were some combinations of wind speed and fire geometry that did induce interaction between the fire fronts and pulled hot gases over an unforested mesa top. In general, the likelihood of this behavior increased with the presence of fire on the mesa top upwind of TA-54 and with the fires in the bottom of the canyon spreading only toward the mesa (not spreading towards and away from the mesa with two diverging firelines). The influence of wind speed on the interaction between the firelines depended on the fire geometry. The highest heat fluxes to areas of interest on top of the mesa in this scoping study occurred when the pre-existing-fire-perimeter was U-Shaped (parallel lines in the canyon bottom and upwind line of fire connecting them by crossing over the top of the mesa).

Realistic vegetation and topography were used to simulate fire scenarios at TA-54. Initially these simulations used a U-shaped ignition similar to those tested in the scoping study. Three different wind speeds were tested for completeness. The highest heat fluxes were seen in a case where the ambient wind was low, but the fires approaching from the south and north arrived at different times. Thus, an additional simulation was performed in order to understand the potential impact of changing the timing of the fire fronts arrival. In this simulation an additional line of fire was implemented in one of the side canyons to the south of TA-54-0375. The presence of this additional fire line caused the fire fronts to converge on building 0375 at similar times and the peak heat flux increased. However, the duration of the significant heat flux was still on the order of hundreds of seconds. The heat fluxes from these calculations were comparable to those measured in the context of a brush fire on a steep slope.

Based on examination of the velocity fields and thermal environment from the realistic simulations of converging lines at TA-54, it was decided that a very long and continuous line of fire in the canyon to the north of TA-54 could potentially pose a similar threat to the Perma-Con if driven by a strong wind. Thus, an additional simulation was performed with this scenario. The magnitude of the heat fluxes was similar to those seen in the U-shaped converging line scenario but the duration of the high heat flux was slightly longer. Thus, the conditions that should be used for detailed analysis of the heat transfer are: 1) the thermal environment from the U-shaped ignition with the extra spur ignition in the side canyon as this scenario gave the maximum heat flux and 2) the thermal environment from the long fireline North of TA-54 with a wind from the Northwest as this gave a longer duration of the high heat flux.

The heat fluxes from these simulations were provided for a detailed calculation of the heat transfer within the Perma-Con. These detailed calculations (described in a companion report) showed that the thermal environment of the Perma-Con was above the levels that risk mitigation experts were comfortable with. For this reason, additional calculations were performed using more realistic debris loading within the Perma-Con perimeter and accounting for the fact that the grass and shrubs will be mowed during fire season. Performing these calculations with this mitigation effort in place, with a refined radiation calculation to handle the larger distances between intense fires and the Perma-Con, provided a thermal environment for the Perma-Con that was deemed acceptable to risk mitigation experts. These calculations are still considered conservative in terms of the simulated wildland fuels in the canyons since these loads are higher than those of the managed fuels that are now in place.

References

Bossert, JE, Linn, RR, Reisner, JM, Winterkamp, JL, Dennison, P, Roberts, D, Ams (2000) 'Coupled atmosphere-fire behavior model sensitivity to spatial fuels characterization.'

Dupuy, JL, Linn, RR, Konovalov, V, Pimont, F, Vega, JA, Jimenez, E (2011) Exploring three-dimensional coupled fire-atmosphere interactions downwind of wind-driven surface fires and their influence on backfires using the higrad-firetec model. *INTERNATIONAL JOURNAL OF WILDLAND FIRE* **20**, 734-750.

Frankman, D, Webb, BW, Butler, BW, Jimenez, D, Forthofer, JM, Sopko, P, Shannon, KS, Hiers, JK, Ottmar, RD (2013) Measurements of convective and radiative heating in wildland fires. *INTERNATIONAL JOURNAL OF WILDLAND FIRE* **22**, 157-167.

Hall, K (2015) Wildland fire exposure evaluation for building ta-54-0375. Los Alamos National Laboratory AP-FIRE-001-FM1, Los Alamos, NM.

Heller, A, Bradley, MM, 2002. This model can take the heat. Science & Technology Review. Lawrence Livermore National Laboratory, Lawrence Livermore National Laboratory. November 2002: 36.

Incropera, FP, DeWitt, DP (2002) 'Fundamentals of heat and mass transfer.' (Wiley: New York)

Linn, R, Anderson, K, Winterkamp, J, Brooks, A, Wotton, M, Dupuy, J-L, Pimont, F, Edminster, C (2012a) Incorporating field wind data into firetec simulations of the international crown fire modeling experiment (icfme): Preliminary lessons learned. *Canadian Journal of Forest Research-Revue Canadienne De Recherche Forestiere* **42**, 879-898.

Linn, RR, Canfield, JM, Cunningham, P, Edminster, C, Dupuy, JL, Pimont, F (2012b) Using periodic line fires to gain a new perspective on multi-dimensional aspects of forward fire spread. *Agricultural and Forest Meteorology* **157**, 60-76.

Linn, RR, Cunningham, P (2005) Numerical simulations of grass fires using a coupled atmosphere–fire model: Basic fire behavior and dependence on wind speed. *Journal of Geophysical Research* **110**, D13107.

Linn, RR, Sieg, CH, Hoffman, CM, Winterkamp, JL, McMillin, JD (2013) Modeling wind fields and fire propagation following bark beetle outbreaks in spatially-heterogeneous pinyon-juniper woodland fuel complexes. *Agricultural and Forest Meteorology* **173**, 139-153.

Linn, RR, Winterkamp, J, Colman, JJ, Edminster, C, Bailey, JD (2005) Modeling interactions between fire and atmosphere in discrete element fuel beds. *INTERNATIONAL JOURNAL OF WILDLAND FIRE* **14**, 37-48.

Raupach, MR, Bradley, EF, Ghadiri, H, 1987. A wind tunnel investigation into aerodynamic effect of forest clearing on the nesting of abbott's boody on christmas island. Csiro Centre for Environmental Mechanics, Canberra.

Reisner, J, Wynne, S, Margolin, L, Linn, R (2000) Coupled atmospheric-fire modeling employing the method of averages. *Monthly Weather Review* **128**, 3683-3691.

Shaw, RH, Denhartog, G, Neumann, HH (1988) Influence of foliar density and thermal-stability on profiles of reynolds stress and turbulence intensity in a deciduous forest. *Boundary-Layer Meteorology* **45**, 391-409.